nature cell biology

Crosstalk between Arg 1175 methylation and Tyr 1173 phosphorylation negatively modulates EGFR-mediated ERK activation

Jung-Mao Hsu[1,2], Chun-Te Chen[1,2,8], Chao-Kai Chou[1,2,8], Hsu-Ping Kuo[1,2,8], Long-Yuan Li[3,4,5], Chun-Yi Lin[3,4], Hong-Jen Lee[1,2], Ying-Nai Wang[1], Mo Liu[1,2], Hsin-Wei Liao[1,2], Bin Shi[1], Chien-Chen Lai[6], Mark T. Bedford[7], Chang-Hai Tsai[5,6] and Mien-Chie Hung[1,2,3,4,5,9]

Epidermal growth factor receptor (EGFR) can undergo post-translational modifications, including phosphorylation, glycosylation and ubiquitylation, leading to diverse physiological consequences and modulation of its biological activity. There is increasing evidence that methylation may parallel other post-translational modifications in the regulation of various biological processes. It is still not known, however, whether EGFR is regulated by this post-translational event. Here, we show that EGFR Arg 1175 is methylated by an arginine methyltransferase, PRMT5. Arg 1175 methylation positively modulates EGF-induced EGFR trans-autophosphorylation at Tyr 1173, which governs ERK activation. Abolishment of Arg 1175 methylation enhances EGF-stimulated ERK activation by reducing SHP1 recruitment to EGFR, resulting in augmented cell proliferation, migration and invasion of EGFR-expressing cells. Therefore, we propose a model in which the regulatory crosstalk between PRMT5-mediated Arg 1175 methylation and EGF-induced Tyr 1173 phosphorylation attenuates EGFR-mediated ERK activation.

EGFR is a transmembrane cell-surface receptor of the ErbB receptor tyrosine kinase family, which converts extracellular cues into intracellular effectors, triggering appropriate cellular responses[1–3]. The biological activity of EGFR is extensively regulated by post-translational modifications[4]. Ligand-induced tyrosine autophosphorylation mediates the initiation of EGFR downstream signalling pathways. *N*-glycosylation of the extracellular domain is important for the membrane transport and maturation of nascent receptor and ligand binding activity of the mature surface receptor. Serine/threonine phosphorylation by protein kinase C (PKC), mitogen-activated protein kinase (MAPK) and calcium/calmodulin-dependent protein kinase II (CaMKII) modulates receptor tyrosine kinase activity and internalization. Cbl-mediated multiple polyubiquitylation regulates EGFR degradation and controls the duration of EGFR activation.

Recent evidence indicates that protein methylation, similarly to other types of post-translational modification, has significant biological functions[5]. Methylation at lysine and arginine residues has been linked to transcription regulation, RNA metabolism, DNA damage repair and signal transduction. As protein methylation comes of age, it is of interest to investigate whether EGFR is regulated by this post-translational modification.

To determine whether EGFR is methylated, we carried out *in vivo* methylation assays. A431 cells were metabolically labelled with L-[methyl-^{3}H]methionine in the presence of protein synthesis inhibitors (Fig. 1a, lanes 1–6), and methylation was detected by fluorography. One radioactive signal corresponding to the molecular weight of EGFR could be detected in the immunoprecipitates of anti-EGFR antibody (lane 2), but not in those of the control antibody (lane 1). Simultaneously, metabolic labelling using L-[^{35}S]methionine was carried out in parallel to monitor the activity of protein synthesis inhibitors (lanes 7–10). The absence of L-[^{35}S]methionine incorporation in the presence of the inhibitors (compare lane 10 with lane 9) indicated that the radiolabelling in lane 2 was the result of post-translational modification and not translational incorporation. Collectively, these findings indicate that EGFR is methylated. To further confirm EGFR methylation and identify methylation site(s), mass spectrometry was

[1]Department of Molecular and Cellular Oncology, The University of Texas MD Anderson Cancer Center, Houston, Texas 77030, USA. [2]The University of Texas Graduate School of Biomedical Sciences at Houston, Houston, Texas 77030, USA. [3]Center for Molecular Medicine, China Medical University Hospital, Taichung 404, Taiwan. [4]Graduate Institute of Cancer Biology, China Medical University, Taichung 404, Taiwan. [5]Department of Biotechnology, Asia University, Taichung 413, Taiwan. [6]Department of Medical Research, China Medical University Hospital, Taichung 404, Taiwan. [7]Science Park-Research Division, The University of Texas MD Anderson Cancer Center, Smithville, Texas 78957, USA. [8]These authors contributed equally to this work.
[9]Correspondence should be addressed to M-C.H. (e-mail: mhung@mdanderson.org)

Received 15 October 2010; accepted 23 November 2010; published online 23 January 2011; DOI: 10.1038/ncb2158

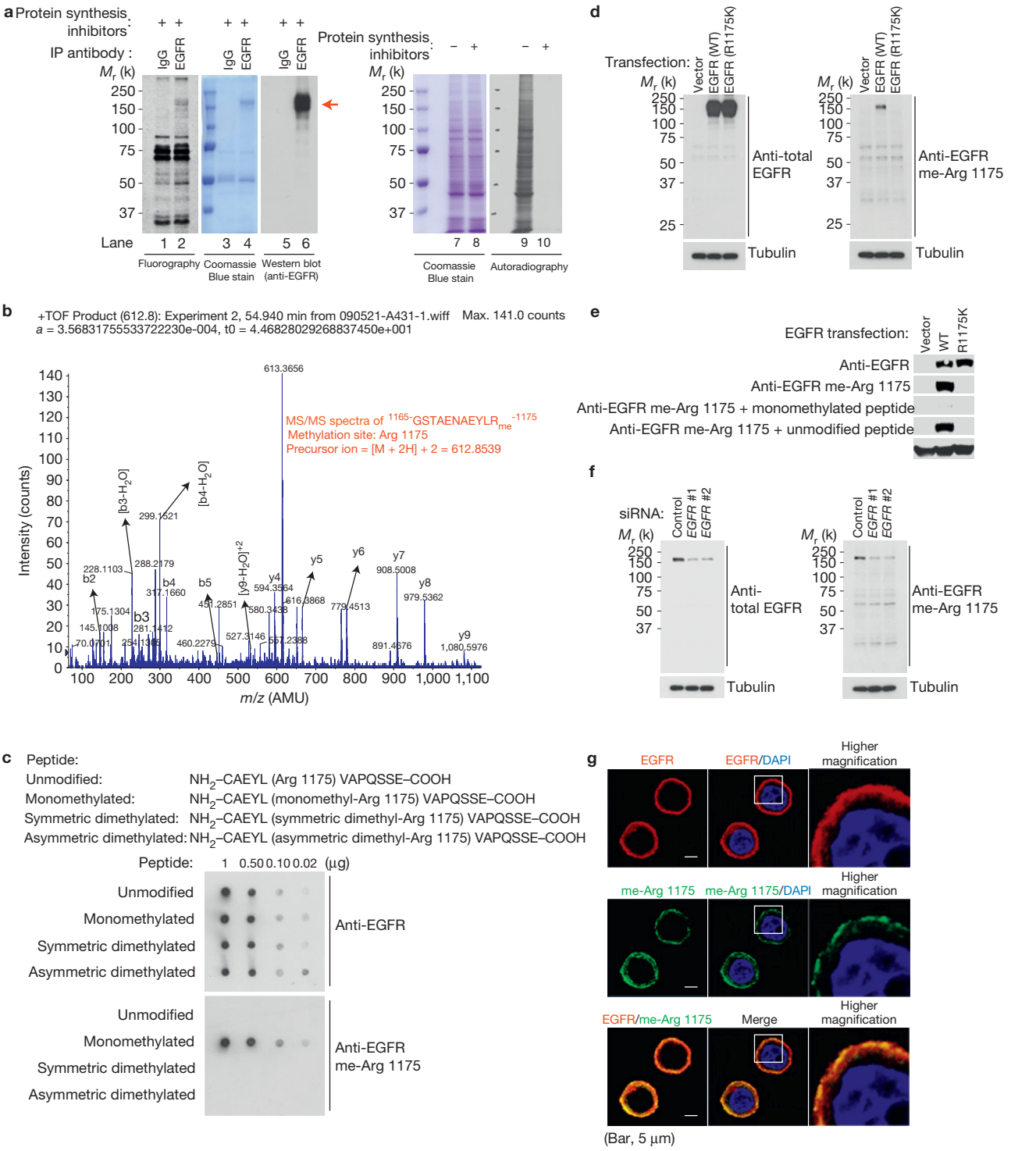

Figure 1 EGFR Arg 1175 is monomethylated. (**a**) *In vivo* methylation of EGFR. A431 cells were metabolically labelled with L-[methyl-^{3}H]methionine (left) or L-[^{35}S]methionine (right) in the presence or absence of protein synthesis inhibitors, as indicated. Immunoprecipitates (IP) of EGFR or control antibodies from L-[methyl-^{3}H]methionine-labelled cells were analysed by fluorography (lanes 1 and 2), Coomassie Blue staining (lanes 3 and 4) or western blotting with EGFR antibody (lanes 5 and 6). Whole-cell lysates of L-[^{35}S]methionine-labelled cells were analysed by Coomassie Blue staining (lanes 7 and 8) or autoradiography (lanes 9 and 10). (**b**) Mass spectrometry analysis of endogenous EGFR immunopurified from A431 cells. (**c**) Amino acid sequence of peptides corresponding to the EGFR 1171–1182 region, in which Arg 1175 is unmodified, monomethylated or dimethylated. Different amounts of peptides were spotted on PVDF membranes and detected by anti-EGFR or anti-EGFR methylated-Arg 1175 (me-Arg 1175) antibodies. (**d**) Western blot analysis of exogenous EGFR in HEK293 cells transfected with control vector, EGFR (WT) or EGFR (R1175K). (**e**) Western blot analysis of exogenous EGFR in HEK293 cells transfected with empty vector, EGFR (WT) or EGFR (R1175K). Anti-EGFR methylated-Arg 1175 antibody was pre-incubated with peptides, as indicated before use. (**f**) Western blot analysis of endogenous EGFR in MDA-MB-468 cells transfected with control or *EGFR* siRNAs. (**g**) Confocal microscopy analysis of MDA-MB-468 cells stained with total endogenous EGFR (red), methylated-Arg 1175 (green) and DAPI (blue). The third columns shows higher-magnification images of the areas outlined in the second column.

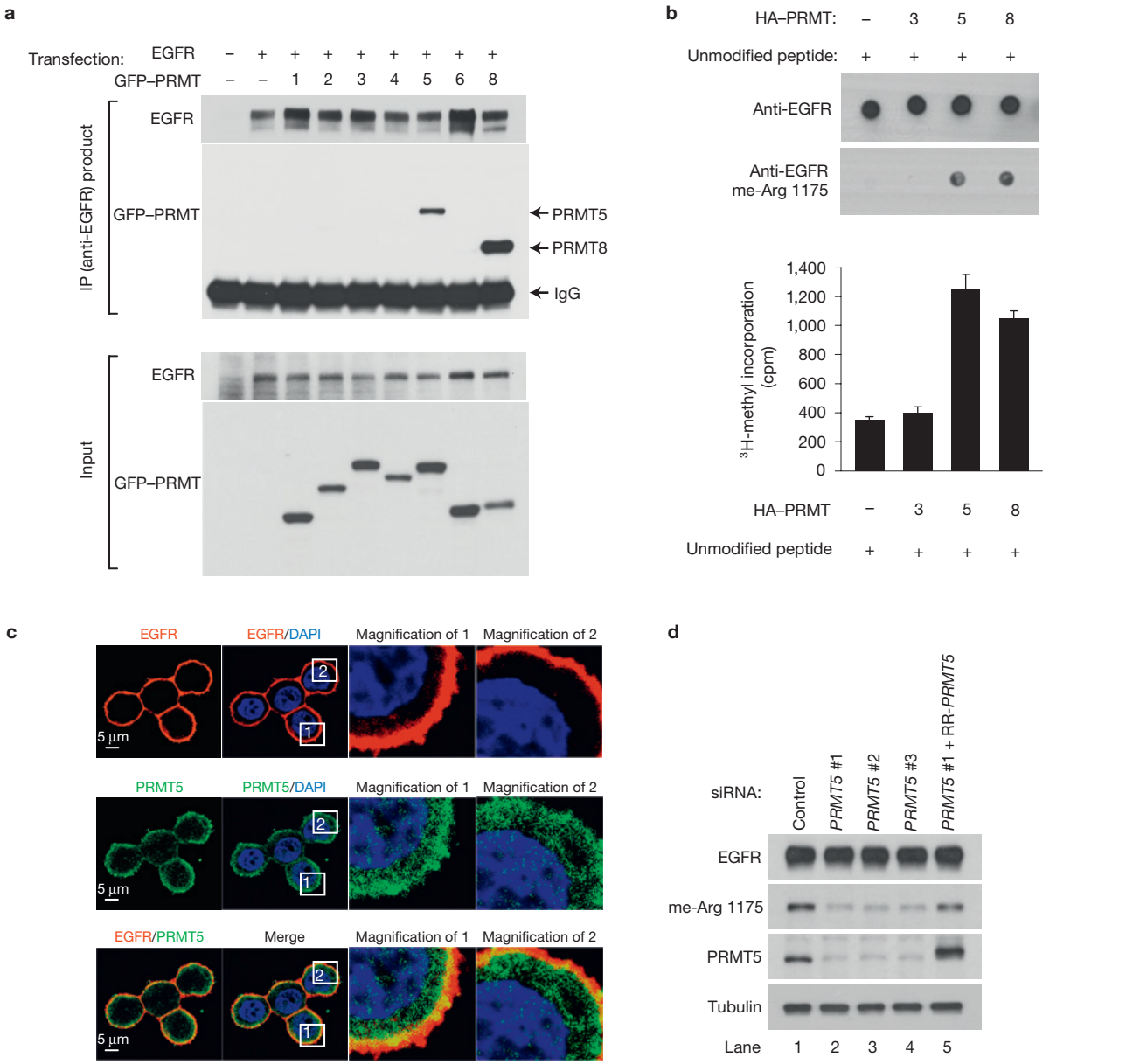

Figure 2 PRMT5 interacts with EGFR and methylates Arg 1175. (**a**) Western blot analysis of exogenous EGFR and PRMTs in the input and anti-EGFR immunoprecipitates from HEK293 cells transfected with EGFR and GFP–PRMTs, as indicated. (**b**) *In vitro* methylation assay of unmodified EGFR peptide by immunopurified HA–PRMT3, 5 or 8. Methylation of peptides was detected by western blotting (top) and scintillation counting (bottom). Error bars represent s.d. ($n = 3$). (**c**) Confocal microscopy analysis of MDA-MB-468 cells stained with endogenous EGFR (red), PRMT5 (green) and DAPI (blue). (**d**) Western blot analysis of endogenous EGFR and total PRMT5 of the MDA-MB-468 cells in which endogenous PRMT5 was knocked down by three *PRMT5* siRNAs (lanes 1–4) and then rescued with an siRNA-resistant *PRMT5* mutant (RR-*PRMT5*; lane 5).

used to analyse endogenous EGFR immunopurified from A431 cells and the result shows that EGFR Arg 1175 is monomethylated (Fig. 1b).

To facilitate detection of EGFR Arg 1175 monomethylation, we raised a polyclonal antibody that specifically recognizes a monomethylated peptide corresponding to the EGFR amino acid 1171–1182 region where Arg 1175 is monomethylated, but not unmodified and dimethylated peptides (Fig. 1c and Supplementary Fig. S1a). Moreover, this antibody recognized only ectopic full-length EGFR wild type (WT) and not the methylation-site mutant (R1175K) in cells (Fig. 1d). In peptide competition assays, the antibody activity was neutralized only by the monomethylated EGFR peptide (Fig. 1e and Supplementary Fig. S1b). Thus, this antibody specifically recognizes Arg-1175-methylated EGFR. In addition to ectopic EGFR proteins, the antibody works well in endogenous EGFR detection (Fig. 1f,g).

Arginine methylation is mediated by enzymes of the protein arginine methyltransferase (PRMT) family[6]. To screen known PRMTs to determine whether they are responsible for EGFR Arg 1175 methylation, we used a co-immunoprecipitation assay to examine whether EGFR physically interacts with PRMT1, 2, 3, 4, 5, 6 or 8. The results indicate that EGFR binds to PRMT5 and PRMT8 (Fig. 2a). Next, *in vitro* methylation assays showed PRMT5 and PRMT8 indeed methylated Arg 1175 of EGFR peptide (Fig. 2b). In human tissues, PRMT5 is ubiquitously expressed, but PRMT8 expression is restricted to the brain[7]. Using confocal immunofluorescence staining, we found that in

breast cancer cells EGFR is mainly associated with the cell membrane region, where some PRMT5 is also found (Fig. 2c). Knockdown of endogenous PRMT5 expression by short interfering RNAs (siRNAs) diminished Arg 1175 methylation, and the phenotype could be rescued by reintroduction of an siRNA-resistant *PRMT5* mutant (RR-*PRMT5*; Fig. 2d). Taken together, these results show that PRMT5 methylates EGFR Arg 1175. Using *in vitro* methylation assays, we further confirmed that Arg 1175 is the only PRMT5 methylation site on EGFR (Supplementary Fig. S1c).

In vitro protein binding assays using recombinant PRMT5 and EGFR proteins indicate that PRMT5 does not directly bind to EGFR (data not shown). Similarly to the interactions between other PRMTs with their substrates[7–9], PRMT5 associates with EGFR mainly through its catalytic core domain (Supplementary Fig. S1d). Moreover, we found that the PRMT5–EGFR association (Supplementary Fig. S2a, top) and the Arg 1175 methylation status (Supplementary Fig. S2a, bottom) remained consistent before and after EGF-mediated EGFR activation, indicating that EGF stimulation and EGFR kinase activity are not required for Arg 1175 methylation.

EGFR signalling is initiated by extracellular ligand binding, which induces activation of the intracellular kinase domain, resulting in trans-autophosphorylation of multiple tyrosine residues in the carboxy-terminal tail region. Phosphotyrosines recruit cytosolic signalling molecules and trigger a series of intracellular pathways, culminating in cell proliferation, migration, invasion and tumourigenicity[1–3]. To investigate whether EGFR Arg 1175 methylation is involved in the EGFR functionality, we generated MCF7 stable transfectants containing EGFR (WT), EGFR (R1175K) or empty vector (designated as MCF7-EGFR (WT), MCF7-EGFR (R1175K) and MCF7-vector, respectively) for serial functional studies (Fig. 3a and Supplementary Fig. S2b). Using 3-(4,5-dimethylthiazol-2-yl)-2,5-diphenyltetrazolium bromide (MTT) colorimetric assays, we observed that MCF7-EGFR (R1175K) cells grew more quickly than MCF7-EGFR (WT) cells (Fig. 3a). Moreover, in an orthotopic breast cancer mouse model, MCF7-EGFR (R1175K) cells proliferated and induced mammary tumour formation more efficiently than MCF7-EGFR (WT) cells (Fig. 3b). In addition, MCF7-EGFR (R1175K) cells also exhibited greater migration (Fig. 3c) and invasion (Fig. 3d) abilities than MCF7-EGFR (WT) cells. These results collectively indicate that Arg 1175 methylation suppresses EGFR functionality.

To further investigate how Arg 1175 methylation affects EGFR functionality, we compared tyrosine phosphorylation of EGF-stimulated EGFR (WT) and EGFR (R1175K) with site-specific antibodies against phospho-Tyr 845, Tyr 992, Tyr 1045, Tyr 1068, Tyr 1086, Tyr 1148 and Tyr 1173. Interestingly, EGF stimulation efficiently induced EGFR (R1175K) phosphorylation at all tyrosine residues tested except Tyr 1173 (Fig. 4a and Supplementary Fig. S2c). To rule out the possibility that the decrease of Tyr 1173 phosphorylation was due to protein conformational misfolding caused by R1175K mutagenesis, we also inhibited EGFR Arg 1175 methylation using multiple *PRMT5* siRNAs as a comparison. Consistently, PRMT5 knockdown specifically downregulated EGF-induced Tyr 1173 phosphorylation and not other tyrosine phosphorylations (Fig. 4b and Supplementary Fig. S2d). These results indicate that Arg 1175 methylation positively modulates Tyr 1173 phosphorylation and are further supported by the *in vitro* kinase assay result that EGFR

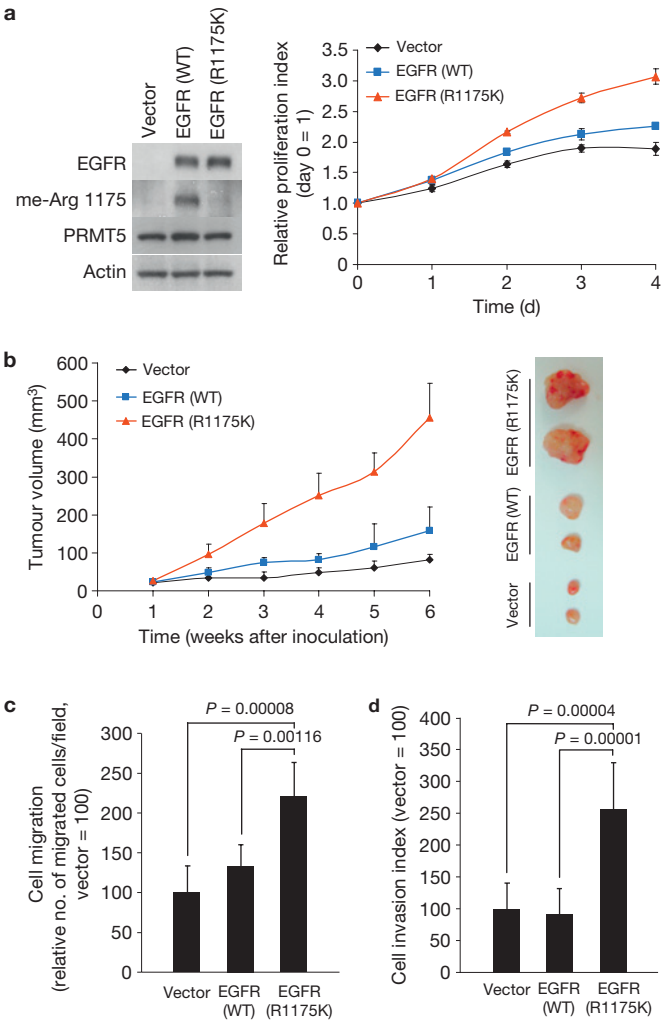

Figure 3 Suppression of Arg 1175 methylation promotes EGFR-mediated cell proliferation, migration and invasion. (**a**) Left: western blot analysis of MCF7 stable transfectants expressing EGFR (WT), EGFR (R1175K) or empty vector. Right: *in vitro* cell proliferation rates were assayed using the MTT colorimetric method. Error bars represent s.d. ($n = 5$). (**b**) Left: *in vivo* cell proliferation was measured using an orthotopic breast cancer mouse model. Error bars represent s.d. ($n = 10$). Right: two representative tumours from each group in the sixth week after inoculation. (**c**) Migration assay of these stable transfectants. Statistical analysis was carried out using Student's *t*-test. Error bars represent s.d. ($n = 3$). (**d**) Invasion assay of these stable transfectants. Statistical analysis was carried out using Student's *t*-test. Error bars represent s.d. ($n = 3$).

phosphorylated the monomethylated peptide more efficiently than the unmodified peptide (Fig. 4c).

Phospho-Tyr 1173 serves as one of the docking sites for the cytosolic signalling molecules Src homology 2 (SH2)-domain-containing transforming protein (SHC) and growth factor receptor-bound protein 2 (Grb2). Recruitment of SHC and Grb2 to EGFR elicits extracellular signal-regulated kinase (ERK) activation[10–12]. Phospho-Tyr 1173 is also the main binding site for SH2-domain-containing protein tyrosine phosphatase 1 (SHP1). In contrast, binding of SHP1 to EGFR results in attenuation of EGFR-dependent ERK activation[13]. As Arg 1175 methylation positively regulates Tyr 1173 phosphorylation, we further investigated whether it regulates the association between EGFR and these cytosolic molecules. Using a co-immunoprecipitation

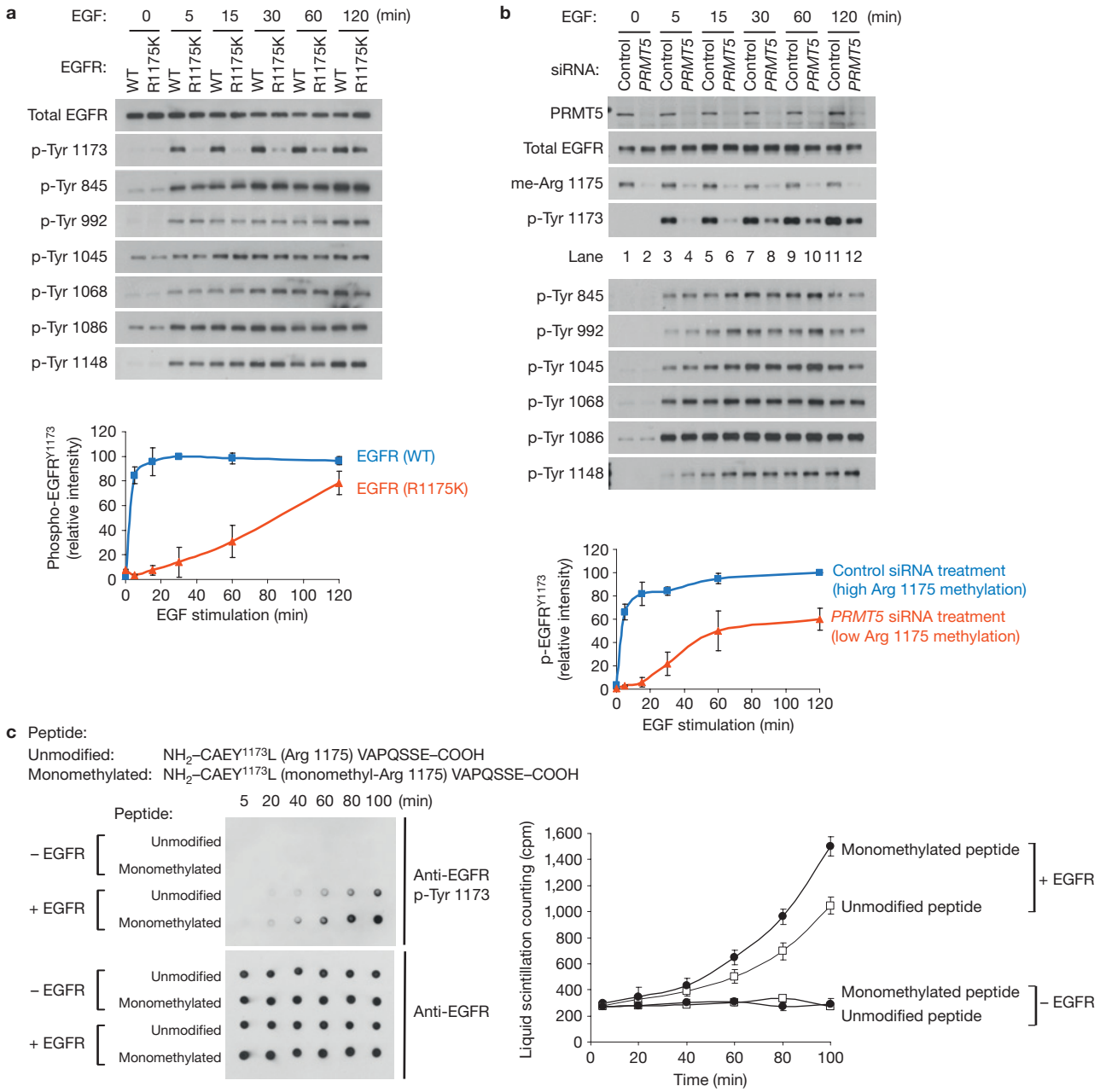

Figure 4 Crosstalk between Arg 1175 methylation and Tyr 1173 phosphorylation. (**a**) Top: western blot analysis of exogenous EGFR in EGF-stimulated MCF7-EGFR (WT) and MCF7-EGFR (R1175K) stable transfectants. Bottom: densitometry of phospho-EGFR Tyr 1173 (p-Tyr 1173) blot. Error bars represent s.d. ($n = 3$). (**b**) Top: western blot analysis of endogenous EGFR in EGF-stimulated MDA-MB-468 cells transfected with control or *PRMT5* siRNA #1. Bottom: densitometry of phospho-EGFR Tyr 1173 (p-Tyr 1173) blot. Error bars represent s.d. ($n = 3$). (**c**) *In vitro* kinase assay of unmodified (open symbols) and monomethylated (filled symbols) EGFR peptides by immunopurified EGFR proteins. Phosphorylation of peptides was detected by western blotting using anti-EGFR phospho-Tyr 1173 antibody (left) and scintillation counting (right). Error bars represent s.d. ($n = 3$).

assay, we found that downregulation of Arg 1175 methylation by R1175K mutagenesis or by *PRMT5* siRNA treatment had no significant effect on EGFR–Grb2 and EGFR–SHC associations, but inhibited EGFR–SHP1 binding (Fig. 5a,b), indicating that Arg 1175 methylation enhances EGFR–SHP1 binding on EGFR activation and may inhibit EGFR-mediated ERK activation.

We also investigated the effect of EGFR Arg 1175 methylation on the activation status of key molecules within four major EGFR downstream signalling pathways, including ERK1 (phospho-ERK1 Thr 202/Tyr 204) and ERK2 (phospho-ERK2 Thr 185/Tyr 187) in the RAS–RAF–MEK–ERK module (RAS, rat sarcoma viral oncogene homologue; RAF, v-raf murine sarcoma viral oncogene homologue; MEK, MAPK/ERK activator kinase), the serine/threonine protein kinase AKT (phospho-AKT Ser 473) in the phosphatidylinositol-3-OH kinase (PI(3)K)–AKT module, phospholipase C (PLC)-γ1 (phospho-PLC-γ1 Thr 783) in the PLC-γ–PKC module, and signal transducer and activator of transcription 3 (STAT3; phospho-STAT3 Thr 705) in the STATs module. Consistently, we found that suppression of

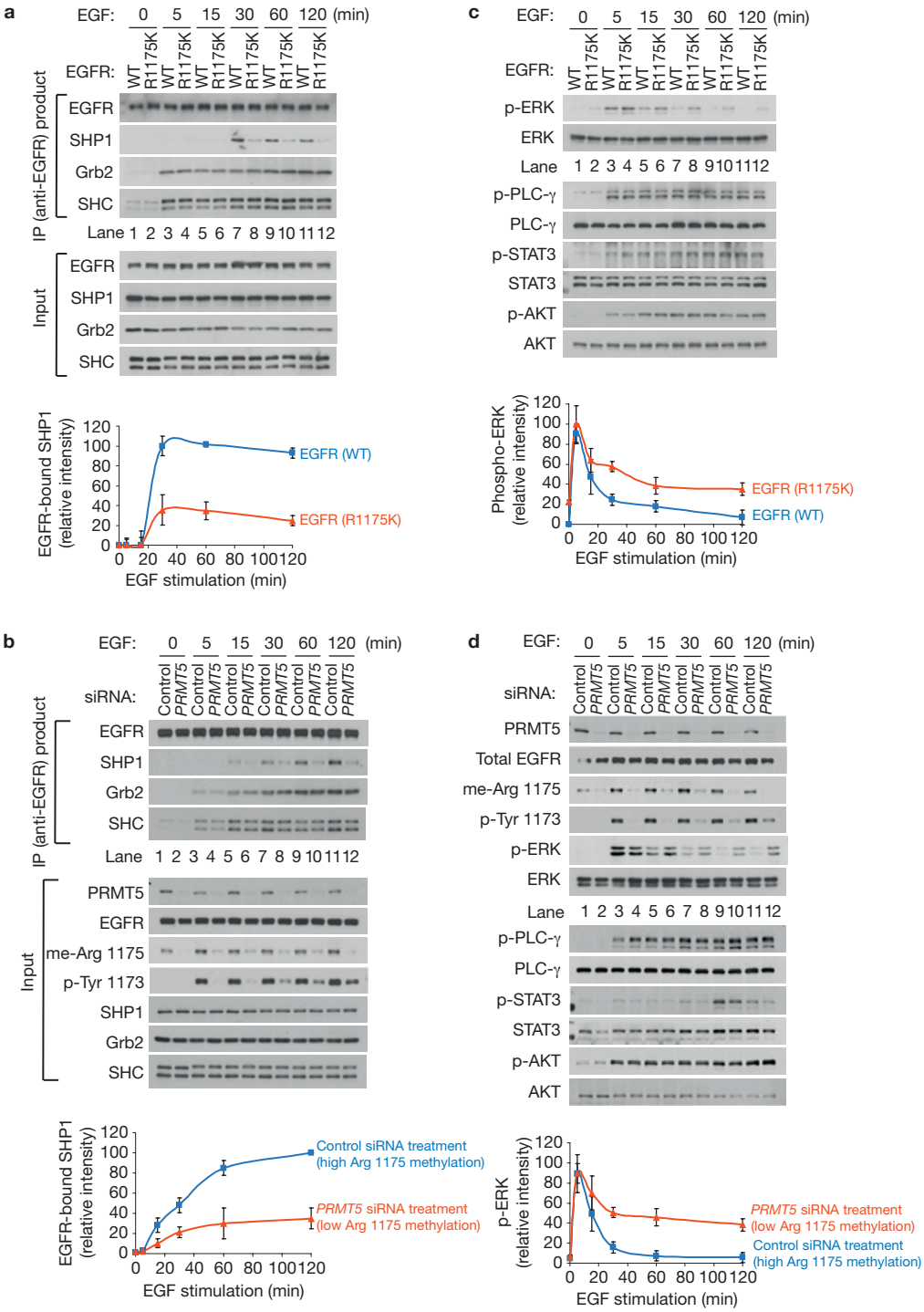

Figure 5 Suppression of Arg 1175 methylation inhibits SHP1 recruitment and prolongs ERK activation. (**a**) Top: western blot analysis of EGFR, SHP1, Grb2 and SHC in the input and anti-EGFR immunoprecipitates from EGF-stimulated MCF7-EGFR (WT) and MCF7-EGFR (R1175K) stable transfectants. Bottom: densitometry of EGFR-bound SHP1 blot. Error bars represent s.d. ($n = 3$). (**b**) Top: western blot analysis of endogenous EGFR, PRMT5, SHP1, Grb2 and SHC in the input and anti-EGFR immunoprecipitates from EGF-stimulated MDA-MB-468 cells transfected with control or *PRMT5* siRNA #1. Bottom: densitometry of EGFR-bound SHP1 blot. Error bars represent s.d. ($n = 3$). (**c**) Top: western blot analysis of endogenous ERK, PLC-γ, STAT3 and AKT in EGF-stimulated MCF7-EGFR (WT) and MCF7-EGFR (R1175K) stable transfectants. Bottom: densitometry of phospho-ERK (p-ERK) blot. Error bars represent s.d. ($n = 3$). (**d**) Top: western blot analysis of endogenous EGFR, PRMT5, ERK, PLC-γ, STAT3 and AKT in EGF-stimulated MDA-MB-468 cells transfected with control or PRMT5 siRNA #1. Bottom: densitometry of phospho-ERK (p-ERK) blot. Error bars represent s.d. ($n = 3$).

Arg 1175 methylation affected only EGFR-mediated activation of ERK (Fig. 5c,d), and not AKT, PLC-γ or STAT3. On EGF treatment, ERK was transiently activated and then rapidly deactivated. Notably, ERK activation status remained higher and lasted longer when EGFR Arg 1175 methylation was suppressed by R1175K mutagenesis or by *PRMT5* siRNA transfection (Fig. 5c,d, compare even lanes and

odd lanes). These results reveal that EGFR Arg 1175 methylation specifically downregulates EGFR-mediated ERK activation. In support of this, ERK inhibitor treatment suppressed the enhanced cell growth, migration and invasion abilities of MCF7-EGFR (R1175K) cells (Supplementary Fig. S3a–c).

In summary, we found that EGFR Arg 1175 methylation positively modulates Tyr 1173 phosphorylation, which enhanced EGFR–SHP1 binding and resulted in suppression of EGFR-mediated ERK activation. This regulatory mechanism indicates that the activation of EGFR downstream pathways could be differentially regulated by EGFR methylation status. Recent identification of histone arginine demethylase indicates that arginine methylation of non-histone proteins may be reversible[14]. Any signalling event leading to a change in Arg 1175 methylation status would specifically modulate the EGF–EGFR–ERK signalling axis. This mechanism also implies the existence of an EGFR protein modification code, which is reminiscent of the histone code encoded by substantially cross-regulated histone modifications[15,16]. In addition to Arg 1175 methylation, we identified seven potential lysine and arginine methylation sites in the kinase domain and C-terminal tail of EGFR (Supplementary Fig. S4a) with some that are close to, or even overlap with, other known modifications (Supplementary Fig. S4b). We predict that further elucidation of the function of individual methylations or the interrelationships between methylations and other modifications would expand our knowledge of the EGFR signalling network.

Moreover, our results provide further evidence showing that the phosphorylation of EGFR on Tyr 1173 has a suppressive effect on ERK signalling. Previous literature gave phospho-Tyr 1173 two opposite roles in EGFR signalling and indicated that Tyr 1173 phosphorylation may cooperate with phospho-Tyr 992, Tyr 1068, Tyr 1086 and Tyr 1148 to elicit ERK signalling through recruitment of SHC and Grb2 (refs 10–12,17), or may work alone to attenuate ERK activation through SHP1 binding[13]. However, to the best of our knowledge, there is no systematic analysis of the interrelationship between these two groups of proteins and phospho-Tyr 1173. Here, we show that EGFR recruitment of these signalling molecules is a time-dependent process. On EGF stimulation, SHC and Grb2 are immediately recruited to EGFR whereas SHP1 binds to EGFR only at the later stage (~30 min later after stimulation). Downregulation of Tyr 1173 phosphorylation diminishes the recruitment only of SHP1, but not SHC or Grb2. These data imply that a main role of Tyr 1173 phosphorylation is to recruit SHP1 at the later stage of EGFR activation to inactivate ERK rather than recruit SHC and Grb2 for ERK activation. The minor effect of phospho-Tyr 1173 downregulation on SHC and Grb2 recruitment could be due to the redundancy in both specificity and function of the different EGFR phosphorylation sites[2,18]. To further address the role of phospho-Tyr 1173 on ERK activation, we made a MCF7-EGFR (Y1173F) stable transfectant and found that it grew faster and exhibited higher tumour formation abilities than the MCF7-EGFR (WT) cells (Supplementary Fig. S3d–f), indicating that phospho-Tyr 1173 has a major suppressive effect on ERK signalling.

The association of SHP1 with EGFR results in suppression of EGFR-mediated ERK activation. However, present knowledge has different interpretations of the action of SHP1 on the EGFR signalling, such that SHP1 binding to the EGFR can cause an overall decrease in tyrosine phosphorylation status of the receptor and attenuation of the receptor signalling both in transient co-expression systems and in stably SHP1-transfected cells[13,19,20]. However, other studies showed that repression of endogenous SHP1 expression by *SHP1* siRNA does not affect full EGFR tyrosine phosphorylation[21]. This contradiction raises the question of how endogenous SHP1 is involved in the EGFR signalling regulation. To clarify this issue, we knocked down endogenous SHP1 expression by *SHP1* siRNA and examined its effect on EGF-stimulated EGFR phosphorylation and downstream signalling activation (Supplementary Fig. S5a). The results show that SHP1 knockdown extends ERK activation and, in line with previous studies, does not affect the EGFR tyrosine phosphorylation status, indicating that endogenous SHP1 may dephosphorylate other molecules rather than EGFR to attenuate ERK activation.

EGFR activates ERK through the EGFR–SHC–Grb2–SOS–RAS–RAF–MEK–ERK pathway (SOS, son of sevenless). On EGF stimulation, the SHC–Grb2–SOS complex is recruited to EGFR. It has been reported that these three molecules are subject to tyrosine phosphorylation[22–24]. Next, we tested whether they are potential targets of SHP1. We found that EGF stimulation induces tyrosine phosphorylation of SHC and SOS, and knockdown of endogenous SHP1 can extend the phosphorylation status of SOS (Supplementary Fig. S5b), indicating that SOS may be a potential target of endogenous SHP1 to reduce the activity of ERK. Given that phospho-Tyr 1173 is the main binding site of SHP1, we further tested whether Tyr 1173 is involved in the regulation of SOS tyrosine phosphorylation, and found SOS phosphorylation status lasted longer in the EGFR (Y1173F) cells than in the EGFR (WT) cells (Supplementary Fig. S5c). Taken together, these data imply that phospho-Tyr 1173 recruits endogenous SHP1 to attenuate ERK activation by reducing the phosphorylation of SOS, rather than EGFR. Moreover, a similar pattern was also observed in the EGFR (R1175K) cells (Supplementary Fig. S5c), further indicating that Arg 1175 methylation downregulates ERK activation by enhancing Tyr 1173 phosphorylation.

Here, we show that EGFR Arg 1175 methylation status is not regulated by EGF stimulation. During the preparation of this manuscript, other studies showed that PRMT5 methyltransferase activity is regulated by methylosome protein 50 (Mep50), whose binding to PRMT5 is required for the methyltransferase activity of PRMT5 (refs 25,26). Mep50 exhibits distinctive subcellular distribution patterns in different pathological stages of breast cancer[27]. In malignant breast epithelia, Mep50 is expressed in the nucleus, whereas in their benign counterparts, Mep50 prefers cytoplasmic localization, which has been demonstrated to inhibit cell growth[27]. However, the mechanism is unclear. As our data support a model in which methylation of EGFR by PRMT5 suppresses cell growth, it is possible that cytoplasmic Mep50 inhibits cell growth through PRMT5-mediated EGFR methylation. To this end, we tested whether cytoplasmic expression of Mep50 upregulates EGFR methylation, and found ectopic expression of nuclear exporting signal (NES)-fused Mep50, rather than nuclear localization signal (NLS)-fused Mep50, increased EGFR Arg 1175 methylation in the MCF7-EGFR (WT) cells (Supplementary Fig. S5d), indicating that cytoplasmic Mep50 can upregulate EGFR Arg 1175 methylation. Next, we evaluated the role of EGFR methylation in cytoplasmic Mep50-mediated cell growth suppression. MCF7-EGFR (WT) cells but not MCF7-EGFR (R1175K) cells were sensitive to NES–Mep50-mediated cell growth suppression (Supplementary Fig. S5e), indicating that

cytoplasmic Mep50 may inhibit cell growth by upregulating EGFR Arg 1175 methylation. Collectively, these data indicate that EGFR Arg 1175 methylation could be regulated by the subcellular distribution of Mep50, and future work will be directed towards elucidation of the role of EGFR methylation in different pathological stages of breast cancer. □

METHODS

Methods and any associated references are available in the online version of the paper at http://www.nature.com/naturecellbiology/

Note: Supplementary Information is available on the Nature Cell Biology website

ACKNOWLEDGEMENTS

This work was supported by the National Institute of Health (RO1 109311 and PO1 099031), the National Breast Cancer Foundation, The Sister Institution Fund of China Medical University and Hospital/MD Anderson Cancer Center, and grants from the National Science Council (NSC 96-3111-B-039, NSC 95-2311-B-039-002 and NSC 99-2632-B-039-001), the National Health Research Institutes (NHRI-EX97-9603BC), and Department of Health (DOH97-TD-G-111-041, DOH97-TD-I-111-TM003 and DOH100-TD-C-111-005) of Taiwan. In memoriam, S. Lin-Guo for her courageous fight against breast cancer.

AUTHOR CONTRIBUTIONS

J-M.H. carried out experimental design and most of the experimental work. J-M.H. and M-C.H. wrote the manuscript. C-K.C. conducted cell migration and invasion experiments. H-P.K. generated stable transfectants and carried out cell proliferation assays. C-T.C. conducted animal experiments. L-Y.L. and C-Y.L. generated antibodies. H-J.L., Y-N.W. and H-W.L. carried out sucrose gradient centrifugation and confocal microscopy analyses. M.L. and B.S. conducted immunoprecipitation assays. C-C.L. carried out mass spectrometry analyses. M.T.B. contributed to PRMT plasmids and reagents. C-H.T. and M-C.H. supervised the project.

COMPETING FINANCIAL INTERESTS

The authors declare no competing financial interests.

Published online at http://www.nature.com/naturecellbiology
Reprints and permissions information is available online at http://npg.nature.com/reprintsandpermissions/

1. Bogdan, S. & Klambt, C. Epidermal growth factor receptor signaling. *Curr. Biol.* **11,** R292–R295 (2001).
2. Citri, A. & Yarden, Y. EGF–ERBB signalling: towards the systems level. *Nat. Rev. Mol. Cell Biol.* **7,** 505–516 (2006).
3. Hynes, N. E. & Lane, H. A. ERBB receptors and cancer: the complexity of targeted inhibitors. *Nat. Rev. Cancer* **5,** 341–354 (2005).
4. Linggi, B. & Carpenter, G. ErbB receptors: new insights on mechanisms and biology. *Trends Cell Biol.* **16,** 649–656 (2006).
5. Paik, W. K., Paik, D. C. & Kim, S. Historical review: the field of protein methylation. *Trends Biochem. Sci.* **32,** 146–152 (2007).
6. Bedford, M. T. Arginine methylation at a glance. *J. Cell Sci.* **120,** 4243–4246 (2007).
7. Bachand, F. Protein arginine methyltransferases: from unicellular eukaryotes to humans. *Eukaryot. Cell* **6,** 889–898 (2007).
8. Pahlich, S., Zakaryan, R. P. & Gehring, H. Protein arginine methylation: cellular functions and methods of analysis. *Biochim. Biophys. Acta* **1764,** 1890–1903 (2006).
9. McBride, A. E. & Silver, P. A. State of the arg: protein methylation at arginine comes of age. *Cell* **106,** 5–8 (2001).
10. Okabayashi, Y. *et al.* Tyrosines 1148 and 1173 of activated human epidermal growth factor receptors are binding sites of Shc in intact cells. *J. Biol. Chem.* **269,** 18674–18678 (1994).
11. Rozakis-Adcock, M. *et al.* Association of the Shc and Grb2/Sem5 SH2-containing proteins is implicated in activation of the Ras pathway by tyrosine kinases. *Nature* **360,** 689–692 (1992).
12. Batzer, A. G., Rotin, D., Urena, J. M., Skolnik, E. Y. & Schlessinger, J. Hierarchy of binding sites for Grb2 and Shc on the epidermal growth factor receptor. *Mol. Cell Biol.* **14,** 5192–5201 (1994).
13. Keilhack, H. *et al.* Phosphotyrosine 1173 mediates binding of the protein-tyrosine phosphatase SHP-1 to the epidermal growth factor receptor and attenuation of receptor signaling. *J. Biol. Chem.* **273,** 24839–24846 (1998).
14. Chang, B., Chen, Y., Zhao, Y. & Bruick, R. K. JMJD6 is a histone arginine demethylase. *Science* **318,** 444–447 (2007).
15. Latham, J. A. & Dent, S. Y. Cross-regulation of histone modifications. *Nat. Struct. Mol. Biol.* **14,** 1017–1024 (2007).
16. Sims, R. J. 3rd & Reinberg, D. Is there a code embedded in proteins that is based on post-translational modifications? *Nat. Rev. Mol. Cell Biol.* **9,** 815–820 (2008).
17. Okutani, T. *et al.* Grb2/Ash binds directly to tyrosines 1068 and 1086 and indirectly to tyrosine 1148 of activated human epidermal growth factor receptors in intact cells. *J. Biol. Chem.* **269,** 31310–31314 (1994).
18. Schulze, W. X., Deng, L. & Mann, M. Phosphotyrosine interactome of the ErbB-receptor kinase family. *Mol. Syst. Biol.* **1,** 2005 0008 (2005).
19. You, M. & Zhao, Z. Positive effects of SH2 domain-containing tyrosine phosphatase SHP-1 on epidermal growth factor- and interferon-gamma-stimulated activation of STAT transcription factors in HeLa cells. *J. Biol. Chem.* **272,** 23376–23381 (1997).
20. Tomic, S. *et al.* Association of SH2 domain protein tyrosine phosphatases with the epidermal growth factor receptor in human tumor cells. Phosphatidic acid activates receptor dephosphorylation by PTP1C. *J. Biol. Chem.* **270,** 21277–21284 (1995).
21. Montano, X. Repression of SHP-1 expression by p53 leads to trkA tyrosine phosphorylation and suppression of breast cancer cell proliferation. *Oncogene* **28,** 3787–3800 (2009).
22. Soler, C., Alvarez, C. V., Beguinot, L. & Carpenter, G. Potent SHC tyrosine phosphorylation by epidermal growth factor at low receptor density or in the absence of receptor autophosphorylation sites. *Oncogene* **9,** 2207–2215 (1994).
23. Li, S., Couvillon, A. D., Brasher, B. B. & Van Etten, R. A. Tyrosine phosphorylation of Grb2 by Bcr/Abl and epidermal growth factor receptor: a novel regulatory mechanism for tyrosine kinase signaling. *EMBO J.* **20,** 6793–6804 (2001).
24. Sini, P., Cannas, A., Koleske, A. J., Di Fiore, P. P. & Scita, G. Abl-dependent tyrosine phosphorylation of Sos-1 mediates growth-factor-induced Rac activation. *Nat. Cell Biol.* **6,** 268–274 (2004).
25. Krause, C. D. *et al.* Protein arginine methyltransferases: evolution and assessment of their pharmacological and therapeutic potential. *Pharmacol. Ther.* **113,** 50–87 (2007).
26. Anne, J. & Mechler, B. M. Valois, a component of the nuage and pole plasm, is involved in assembly of these structures, and binds to Tudor and the methyltransferase Capsuleen. *Development* **132,** 2167–2177 (2005).
27. Peng, Y. *et al.* Androgen receptor coactivator p44/Mep50 in breast cancer growth and invasion. *J. Cell Mol. Med.* **14,** 2780–2789 (2009).

DOI: 10.1038/ncb2158

METHODS

Constructs, antibodies, reagents and peptides. All green fluorescent protein (GFP)–PRMT plasmids were provided by M. T. Bedford. PRMT3, PRMT5 and PRMT8 complementary DNAs were further subcloned into a modified pCMV5 vector containing an N-terminal haemagglutinin (HA) tag. Full-length EGFR cDNA was cloned into a pCDNA3 vector. PRMT5 and EGFR intracellular domain (ICD; amino acids 645–1186) were further subcloned into a modified pCMV5 vector containing an N-terminal glutathione *S*-transferase (GST) tag for the purification of recombinant protein. $EGFR^{R1175K}$ and $PRMT5^{R368A}$ mutageneses were generated using the QuickChange Site-Directed Mutagenesis Kit according to the manufacturer's protocol (Stratagene). Epidermal growth factor (EGF; Sigma) and U0126 (Cell Signaling) were prepared according to the manufacturers' instructions. The following peptides were chemically synthesized by QCB for antibody production in mice, dot blots, peptide competition assays and *in vitro* methylation assays. Unmodified peptide: NH_2–CAEYLRVAPQSSE–COOH; methylated peptides: NH_2–CAEYL(monomethyl-R)VAPQSSE–COOH, NH_2–CAEYL(symmetric dimethyl-R)VAPQSSE–COOH and NH_2–CAEYL(asymmetric dimethyl-R)VAPQSSE–COOH. Histone H4 peptide with monomethyl R3 was purchased from Abcam. Anti-EGFR antibody (Ab-12, 1:5,000; Thermo Scientific) and anti-EGFR antibody (06-847, 1:5,000; Millipore) were used to detect full-length EGFR and EGFR peptides, respectively. For detection of EGFR tyrosine phosphorylations, antibody against phosphotyrosine (4G10, 1:5,000; Millipore) was used to detect total tyrosine phosphorylations, and site-specific antibodies against phospho-Tyr 845, -Tyr 992, -Tyr 1045, -Tyr 1068, -Tyr 1086, -Tyr 1148 and -Tyr 1173 (Cell Signaling and Abcam) were used (1:2,000) to detect individual phosphotyrosines. Antibodies to ERK (1:5,000; Millipore), SHP1 (1:2,000; Millipore) and SHC (1:5,000; Millipore), antibodies to STAT3 (1:2,000; Santa Cruz) and SOS (1:2,000; Santa Cruz), and antibodies to AKT (1:2,000; Cell Signaling), PLC-γ (1:2,000; Cell Signaling), phospho-ERK (1:5,000; Cell Signaling), phospho-AKT (1:2,000; Cell Signaling), phospho-STAT3 (1:2,000; Cell Signaling), phospho-PLC-γ (1:2,000; Cell Signaling) and Grb2 (1:2,000; Cell Signaling) were used to detect the EGFR downstream pathways. Anti-PRMT5 (1:5,000) and anti-tubulin (1:5,000) antibodies were from Sigma. Anti-GFP (1:5,000) antibody was from Thermo Scientific. For immunofluorescence staining, antibodies were diluted 1:200. For immunoprecipitation, 5 μg of anti-EGFR (Ab-13; Thermo Scientific), anti-Grb2, anti-SHC or anti-SOS antibodies were used per 1 mg of total protein in 1 ml of cell lysates.

***In vivo* methylation assay.** For *in vivo* methylation of EGFR, a procedure modified from a previously described method[28] was used. A431 cells were incubated for 1 h in Dulbecco's modified Eagle's medium (DMEM; GIBCO) supplemented with 10% fetal bovine serum (FBS), 100 μg ml^{-1} cycloheximide (Sigma) and 40 μg ml^{-1} chloramphenicol (Sigma). Then, cells were washed twice with methionine-depleted DMEM (GIBCO) and incubated in the same medium containing 10 μCi ml^{-1} L-[methyl-^{3}H]methionine (Amersham Biosciences), 10% dialysed FBS (GIBCO), 100 μg ml^{-1} cycloheximide and 40 μg ml^{-1} chloramphenicol. After labelling for 5 h, endogenous EGFR was immunopurified and analysed by SDS–PAGE. ^{3}H-methyl incorporation was visualized by fluorography. To monitor the effect of protein synthesis inhibitors, A431 cells were also labelled with 10 μCi ml^{-1} L-[^{35}S]methionine (MP Biomedicals) using a procedure almost exactly the same as the one described above, with or without protein synthesis inhibitors. After labelling, whole-cell lysates were prepared, analysed by SDS–PAGE, and detected by autoradiography.

***In vitro* methylation assay.** HA–PRMT3, HA–PRMT5 and HA–PRMT8 were expressed in HEK293 cells and immunopurified using HA–agarose (Sigma). The enzymes immobilized on the beads were then incubated with unmodified peptide (50 μg) in the presence of 2.2 μCi *S*-adenosyl-L-[methyl-^{3}H]methionine (85 Ci mmol^{-1} from a 0.55 mCi ml^{-1} stock solution; MP Biomedicals) for 1 h at 30 °C in a final volume of 50 μl of phosphate-buffered saline (PBS). One microgram of peptide was spotted onto polyvinylidene difluoride (PVDF) membranes and detected using anti-EGFR or anti-EGFR methylated-Arg-1175 antibodies. Five micrograms of peptide was spotted onto P81 papers, washed, and counted by liquid scintillation.

An *in vitro* methylation assay was also carried out as follows. GST–PRMT5 and GST–EGFR (ICD) were expressed in HEK293 cells and purified using glutathione resin (GE Healthcare). GST–PRMT5 and GST–EGFR (ICD) proteins were incubated in the presence of 2.2 μCi *S*-adenosyl-L-[methyl-^{3}H]methionine (85 Ci mmol^{-1} from a 0.55 mCi ml^{-1} stock solution) for 1 h at 30 °C in a final volume of 50 μl PBS. Subsequently, samples were analysed by SDS–PAGE and EGFR methylation was detected using fluorography and anti-EGFR methylated-Arg-1175 antibody.

***In vitro* kinase assay.** A procedure modified from a previously published method[29] was used. HA–EGFR was expressed in HEK293 cells and immunopurified using HA–agarose. The EGFR proteins immobilized on the beads were then incubated with unmodified or monomethylated peptides (50 μg) in a total volume of 50 μl of reaction buffer containing 5 mM HEPES (pH 7.4), 50 μM Na_3VO_4, 5 mM $MgCl_2$, 2 mM $MnCl_2$, 40 μg ml^{-1} bovine serum albumin, 250 mM ammonium sulphate, 25 μM ATP, and 62.5 μCi ml^{-1} [γ-^{32}P]ATP (MP Biomedicals). Reactions were carried out at 30 °C and stopped by using 8.5% phosphoric acid. One microgram of peptide was spotted onto PVDF membranes and detected using anti-EGFR or anti-EGFR phospho-Tyr 1173 antibodies. Five micrograms of peptide was spotted onto P81 papers, washed and counted by liquid scintillation.

siRNA transfection and siRNA-resistant mutant of *PRMT5*. Cells were transfected individually with three *PRMT5* siRNA oligonucleotides (#1: 5′-UGGCACAACUUCCGGACUUUU-3′, #2: 5′-CAACAGAGAUCCUAUGAUU-3′ or #3: 5′-CGAAAUAGCUGACACACUA-3′) or two *EGFR* siRNA oligonucleotides (#1: 5′-CAAAGUGUGUAACGGAAUA-3’ or #2: 5′-CCAUAAAUGCUACGAAUAU-3′) or one *SHP1* siRNA (5′-GGAACAAAUGCGUCCCAUA-3′) with DharmaFECT 1 (Dharmacon), and used for experiments 96 h after transfection. A non-targeting siRNA (5′-UGGUUUACAUGUCGACUAA-3′) was used as control. To rescue the phenotype of *PRMT5* siRNA, an siRNA-resistant mutant of *PRMT5* (RR-*PRMT5*) was created by substituting five nucleotides in the *PRMT5* siRNA #1 targeting region (C570T, C573T, C576T, C577A and G579A).

Mass spectrometry. EGFR was isolated by immunoprecipitation with anti-EGFR antibody and analysed by SDS–PAGE. The protein band corresponding to EGFR was excised and subjected to in-gel digestion with trypsin. After being isolated from the gel, samples were analysed by nanoelectrospray mass spectrometry, using an Ultimate capillary LC system (LC Packings) coupled to a $QSTAR^{XL}$ quadrupole time-of-flight mass spectrometer (Applied Biosystem/MDS Sciex).

Confocal microscopy analysis. Cultured cells were washed three times with PBS, fixed in 4% paraformaldehyde for 15 min, permeabilized with 0.5% Triton X-100 for 15 min, and incubated with 5% bovine serum albumin for 1 h. Cells were then incubated with the primary antibodies overnight at 4 °C. Cells were washed with PBS and then further incubated with the appropriate secondary antibody diluted at 1:500 and tagged with fluorescein isothiocyanate (FITC), Texas Red or Alexa 647 (Molecular Probes) for 45 min at room temperature. Nuclei were stained with 4,6-diamidino-2-phenylindole (DAPI) before mounting. Confocal fluorescence images were captured using a Zeiss LSM710 laser microscope. In all cases, optical sections through the middle planes of the nuclei, as determined using nuclear counterstaining, were obtained.

Cell proliferation assay. Cells (5×10^3 cells per well) were seeded in 96-well plates, and relative cell amounts were determined by the MTT colorimetric method on a daily basis. MTT (Sigma) at 1 mg ml^{-1} was added to each well. After 2-h incubation, the medium was removed, and the MTT was dissolved in 100 μl of dimethylsulphoxide. The absorbance was measured at 570 nm, and the relative proliferation index for each day was determined using the absorbance at day 0 as the standard.

Migration and invasion assay. Cell migration and invasion were analysed using Biocoat Control inserts and Biocoat Matrigel invasion chambers (BD Biosciences), respectively. Cells (2×10^5) in DMEM medium with 0.1% FBS were added to the upper chamber and allowed to penetrate a porous (8 μm), uncoated membrane or a Matrigel-coated membrane to the bottom chamber containing DMEM medium with 10% FBS. Cells on the top surface of the membrane were removed 72 h after incubation, and the remaining cells on the bottom surface were fixed with 4% paraformaldehyde, stained with 0.5% crystal violet and counted from four random fields of each membrane using a bright-field microscope. The average cell number per field for each membrane was used to calculate the mean and s.d. for triplicate membranes. Migration value is shown as 'number of migrated cells per field'. Invasion value is reported as the 'invasion index = number of invaded cells per field/number of migrated cells per field'.

Mouse model. *In vivo* cell growth was analysed in an orthotopic breast cancer mouse model[30]. Briefly, cells (5×10^6 cells) were injected into the mammary fat pads of nude mice, and the tumour volumes were measured weekly.

Statistics. All quantitative results are presented as the mean and s.d. of independent experiments. Statistical differences between two groups of data were analysed by Student's *t*-test.

28. Liu, Q. & Dreyfuss, G. *In vivo* and *in vitro* arginine methylation of RNA-binding proteins. *Mol. Cell Biol.* **15,** 2800–2808 (1995).
29. Lee, J., Sayegh, J., Daniel, J., Clarke, S. & Bedford, M.T. PRMT8, a new membrane-bound tissue-specific member of the protein arginine methyltransferase family. *J. Biol. Chem.* **280,** 32890–32896 (2005).
30. Chang, J. Y. *et al.* The tumor suppression activity of E1A in HER-2/neu-overexpressing breast cancer. *Oncogene* **14,** 561–568 (1997).

nature cell biology

DOI: 10.1038/ncb2158

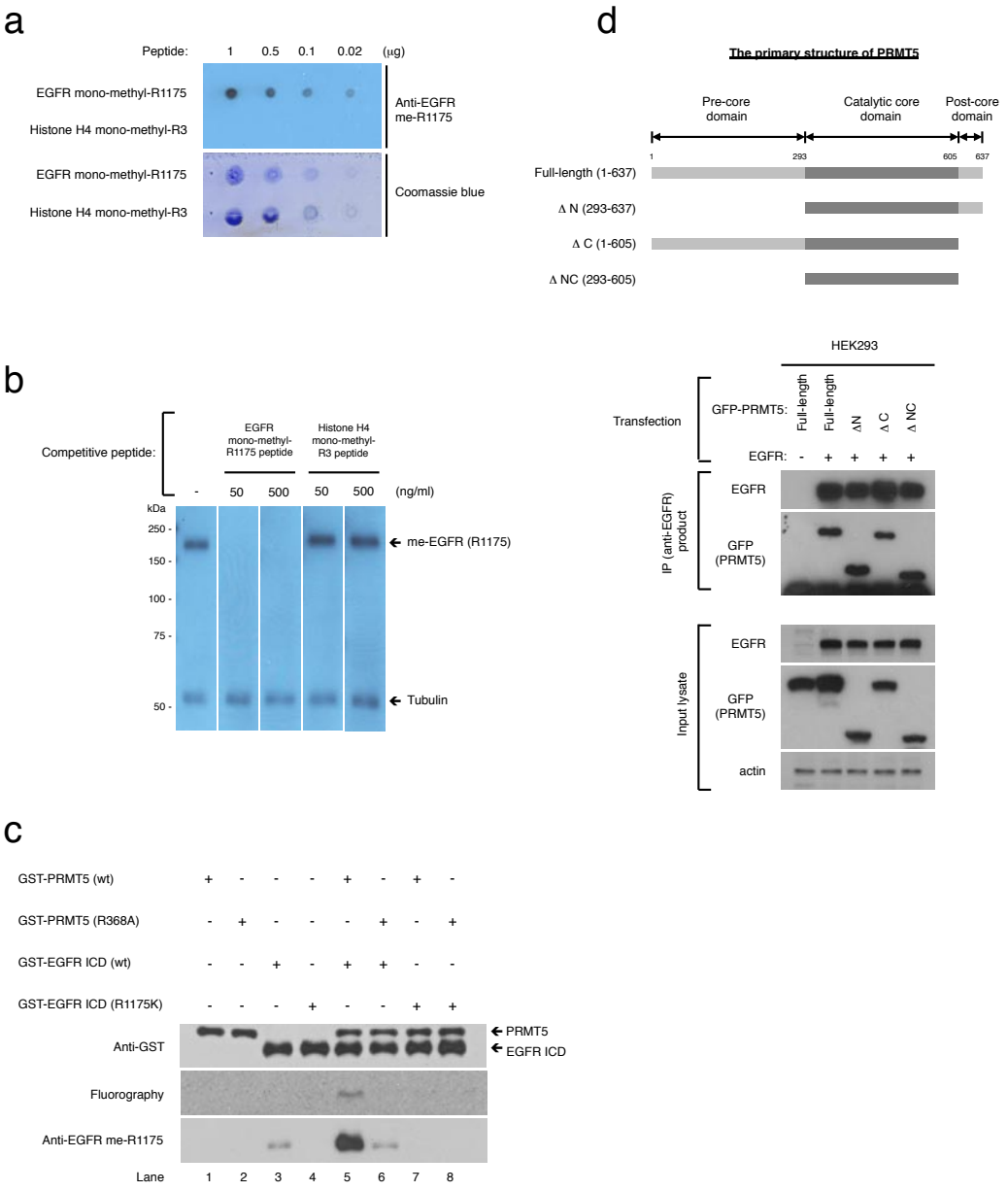

Figure S1 (**a**) Various amounts of the EGFR peptide with monomethyl R1175 or a Histone H4 peptide with monomethyl R3 were spotted on PVDF membranes and detected by anti-EGFR me-R1175 antibody or coomassie blue. (**b**) Western blot analysis of endogenous EGFR in MDA-MB-468 cells. Anti-EGFR me-R1175 antibody was pre-incubated with EGFR or Histone H4 peptides, as indicated prior to use. (**c**) *In vitro* methylation assay of EGFR intracellular domain (ICD) wild type (wt) or R1175K mutant by PRMT5 wild type (wt) or inactive mutant (R368A). Methylation of EGFR (ICD) was detected by fluorography and western blotting using anti-EGFR me-R1175 antibody. (**d**) Top panel: Schematic representation of the PRMT5 domain structure containing catalytic core, pre-core and post-core domains. PRMT5 truncation mutants without pre-core domain, post-core domain or both domains are assigned as ΔN, ΔC or ΔNC, respectively. Alphabets indicate amino acid residues. Bottom panel: Western blot analysis of exogenous EGFR and PRMT5 in the input and anti-EGFR immunoprecipitates from HEK293 cells transfected with EGFR and various PRMT5 truncation mutants.

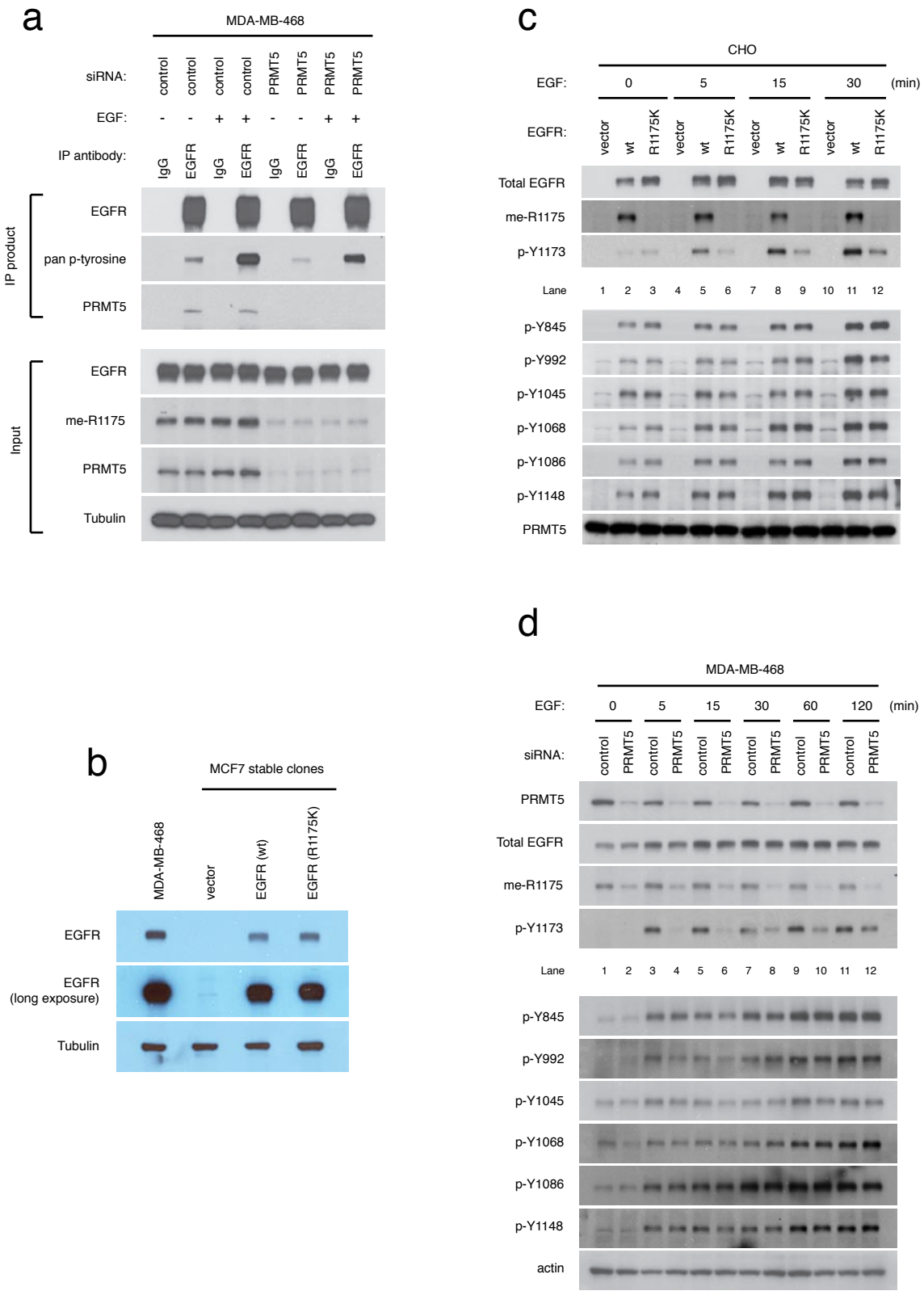

Figure S2 (**a**) Western blot analysis of endogenous EGFR and PRMT5 in the input (bottom panel) and immunoprecipitates of indicated antibodies (top panel) from EGF-stimulated and siRNA-transfected MDA-MB-468 cells. (**b**) Western blot analysis of EGFR expression in MDA-MB-468 cells and the MCF7-EGFR stable transfectants. (**c**) Western blot analysis of exogenous EGFR in EGF-stimulated CHO cells transfected with empty vector, EGFR (wt) or EGFR (R1175K). (**d**) Western blot analysis of endogenous EGFR in EGF-stimulated MDA-MB-468 cells transfected with control or PRMT5 siRNA #2.

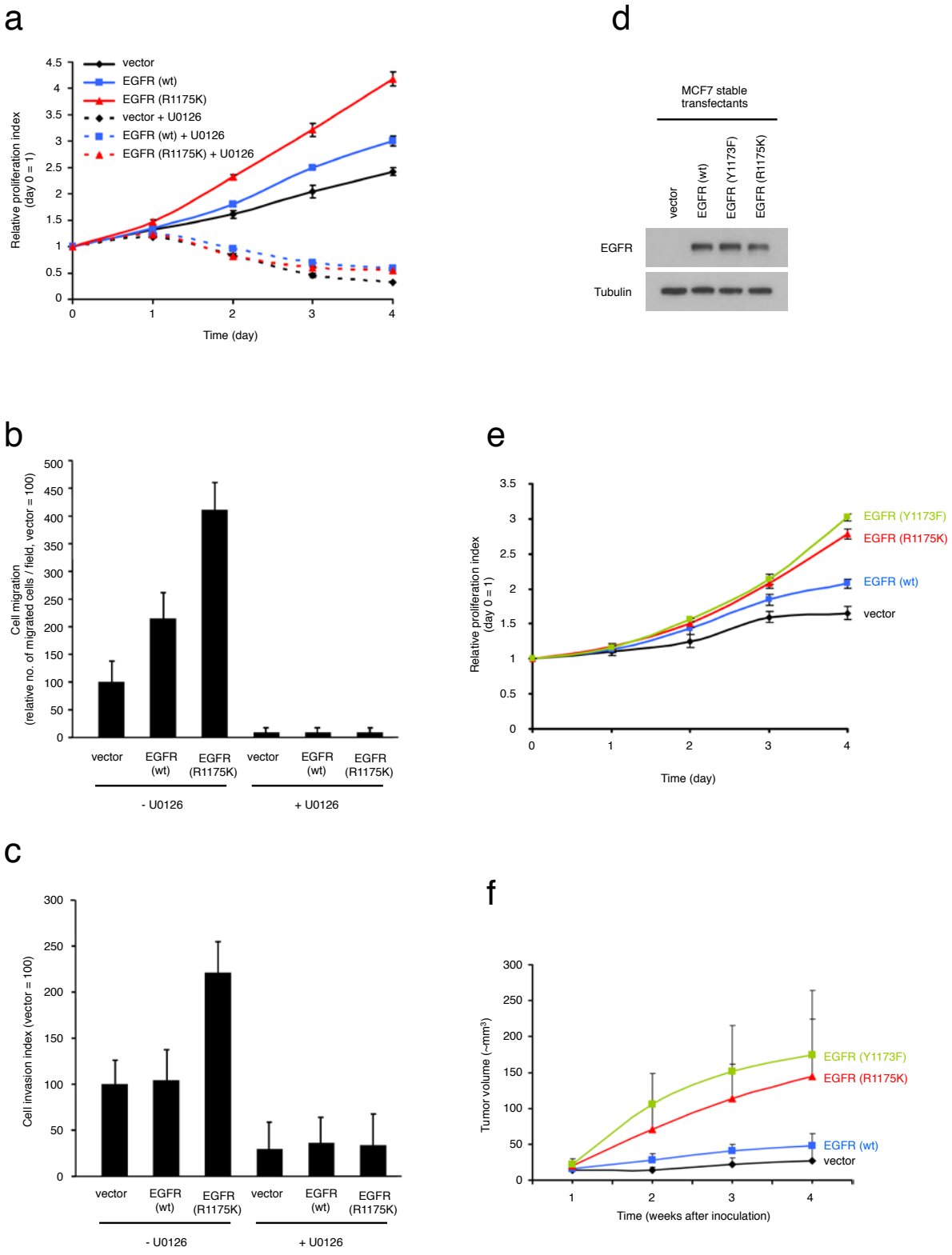

Figure S3 (**a**) *In vitro* cell proliferation, (**b**) migration, and (**c**) invasion assays of MCF-EGFR (wt), MCF-EGFR (R1175K), and MCF7-vector cells were performed in the presence or absence of the ERK inhibitor U0126. Error bars represent s.d. (n = 3). (**d**) Western blot analysis of MCF7 stable transfectants expressing EGFR (wt), EGFR (Y1173F), EGFR (R1175K) or empty vector. (**e**) *In vitro* cell proliferation assay of the stable transfectants using the MTT colorimetric method. Error bars represent s.d. (n = 5). (**f**) *In vivo* cell proliferation of the stable transfectants in an orthotopic breast cancer mouse model. Error bars represent s.d. (n = 10).

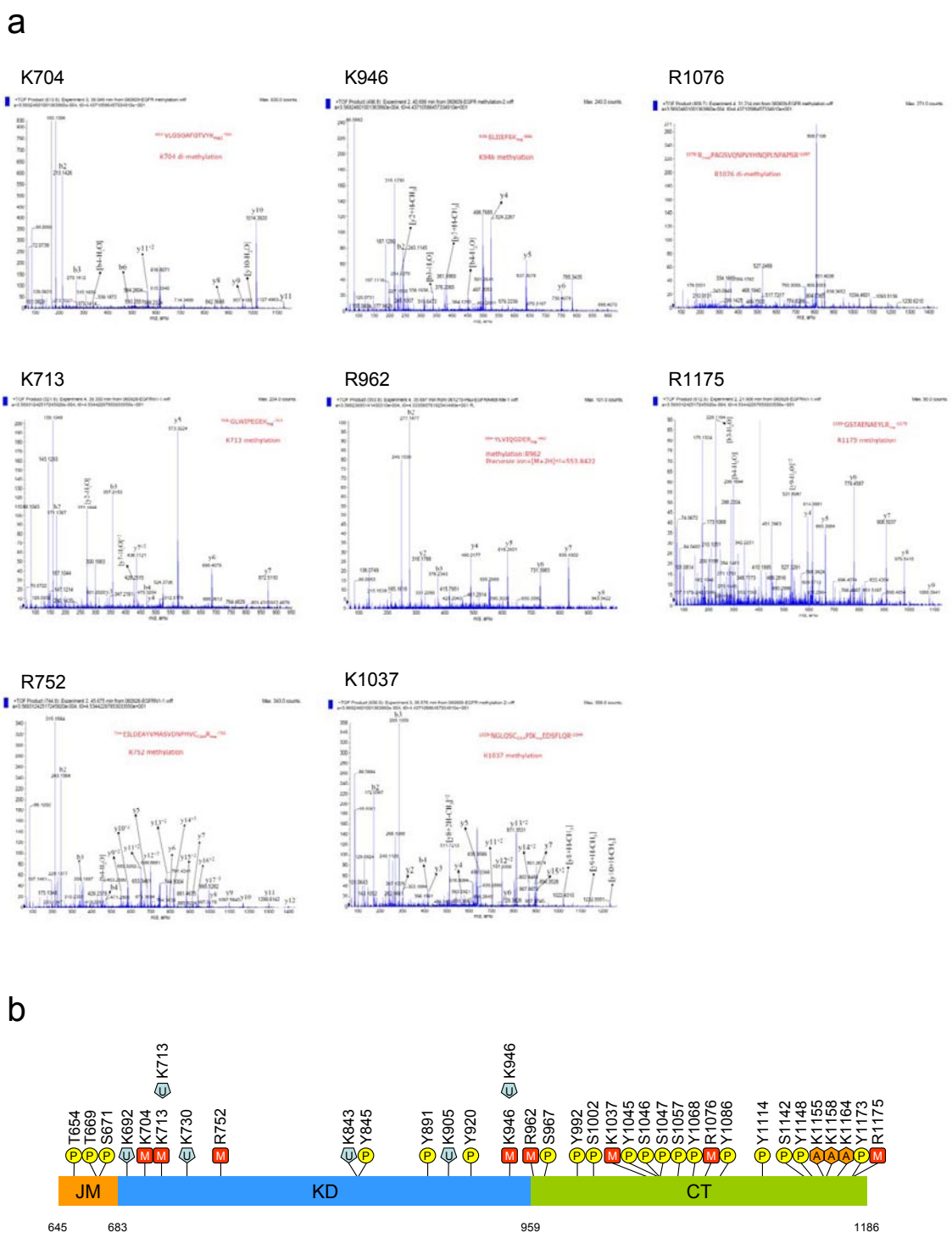

Figure S4 Summary of EGFR post-translational modifications. (**a**) Mass spectrometry identification of EGFR methylation sites. In addition to R1175 monomethylation, another seven potential EGFR methylation sites were identified in our mass spectrometry analysis, including one dimethylated lysine (K704), three monomethylated lysines (K713, K946 and K1037), two monomethylated arginines (R752 and R962) and one dimethylated arginine (R1076). (**b**) Schematic representation of the functional domains of EGFR intracellular domain (amino acid 645-1186), including a juxtamembrane domain (JM, amino acid 645-683), a tyrosine kinase domain (KD, amino acid 683-959) and a C-terminal tail region (CT, amino acid 959-1186). The relative positions of known EGFR post-translational modifications[4, 5], including phosphorylation (P), ubiquitination (U), acetylation (A) and also the methylation (M) sites we identified are indicated. Alphabets indicate the amino acid residues subjected to modifications (T, threonine; S, serine; Y, tyrosine; K, lysine; R, arginine). Arabic numbers indicate amino acid positions.

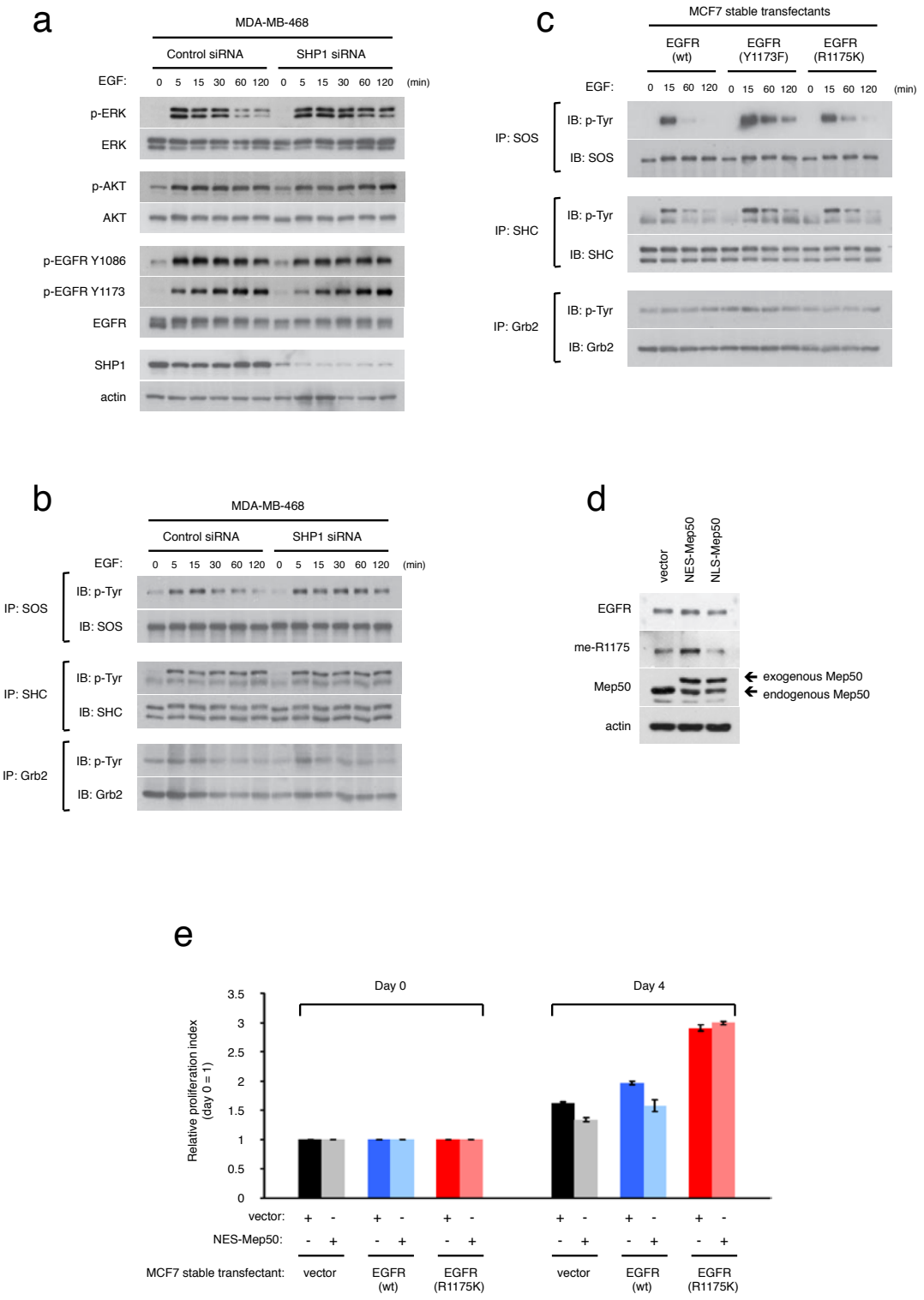

Figure S5 (**a**) Western blot analysis of endogenous EGFR, ERK and AKT in EGF-stimulated MDA-MB-468 cells transfected with control or SHP1 siRNA. (**b**) Western blot analysis of the tyrosine phosphorylation status of SOS, SHC and Grb2 immunoprecipitated from EGF-stimulated MDA-MB-468 cells transfected with control or SHP1 siRNA. (**c**) Western blot analysis of the tyrosine phosphorylation status of SOS, SHC and Grb2 immunoprecipitated from EGF-stimulated MCF7-EGFR (wt), MCF7-EGFR (Y1173F) and MCF7-EGFR (R1175K) stable transfectants. (**d**) Western blot analysis of EGFR and Mep50 in the MCF7-EGFR (wt) cells ectopically expressed with NES (nuclear exporting signal)-fused Mep50, NLS (nuclear localization signal)-fused Mep50, or empty vector. (**e**) *In vitro* cell proliferation assay of the MCF7-EGFR stable transfectants expressed with NES-Mep50 or vector. Error bars represent s.d. (n = 5).

Fig. 2d

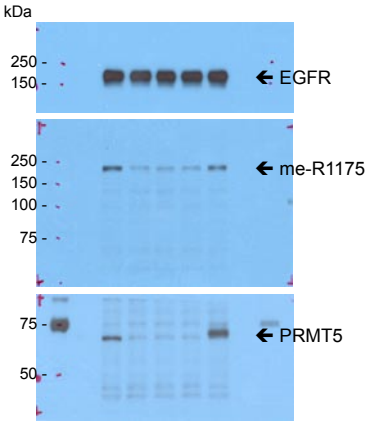

Fig. 4a

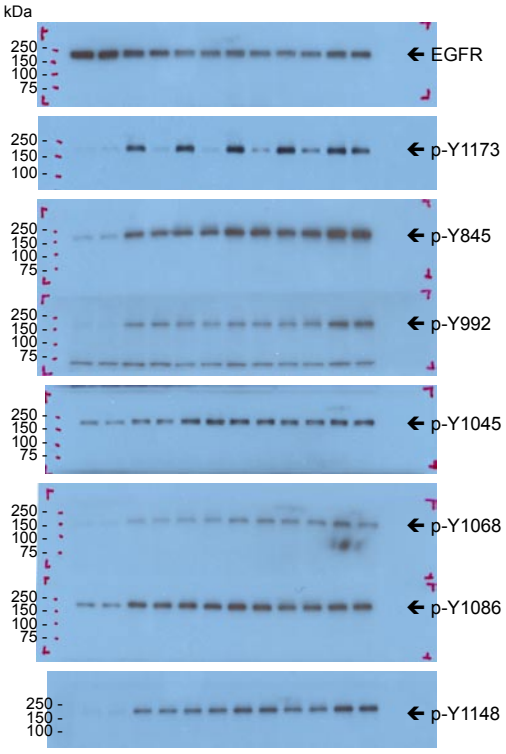

Fig. 4b

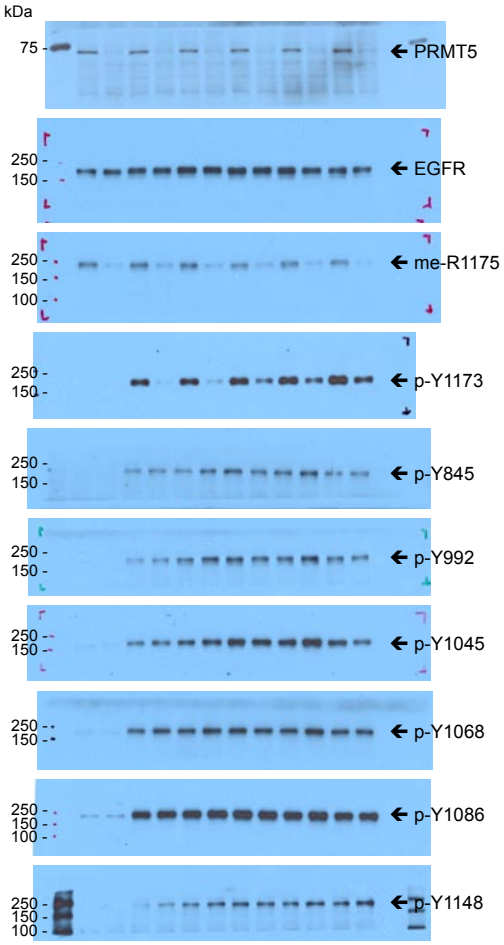

Figure S6 Uncropped key blots.

Fig. 5a

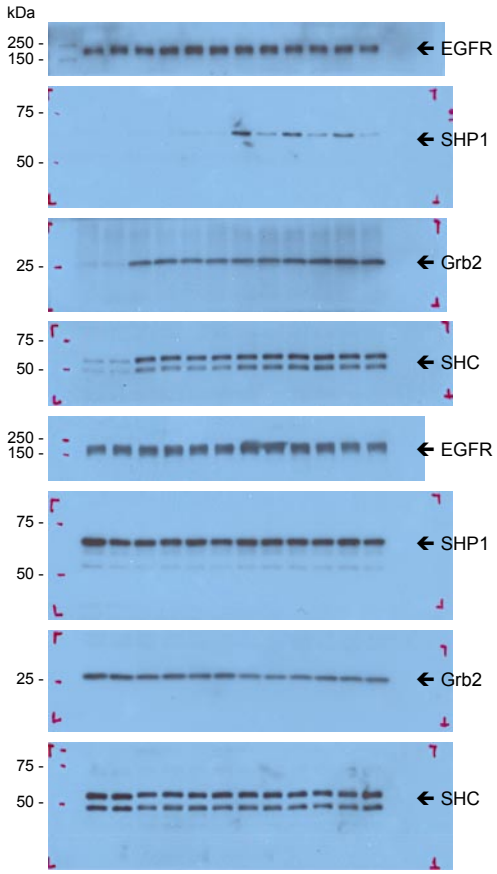

Fig. 5b

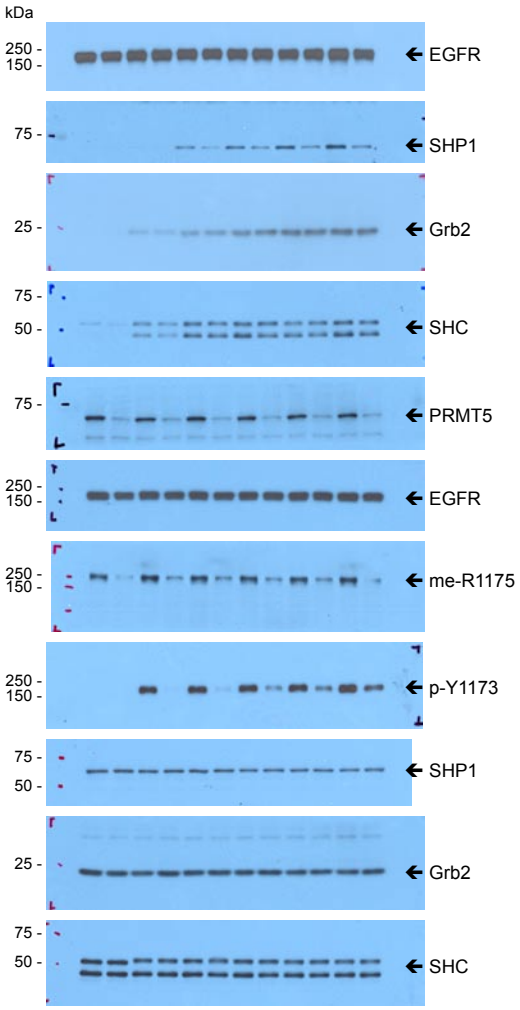

Figure S6 continued

Fig. 5c

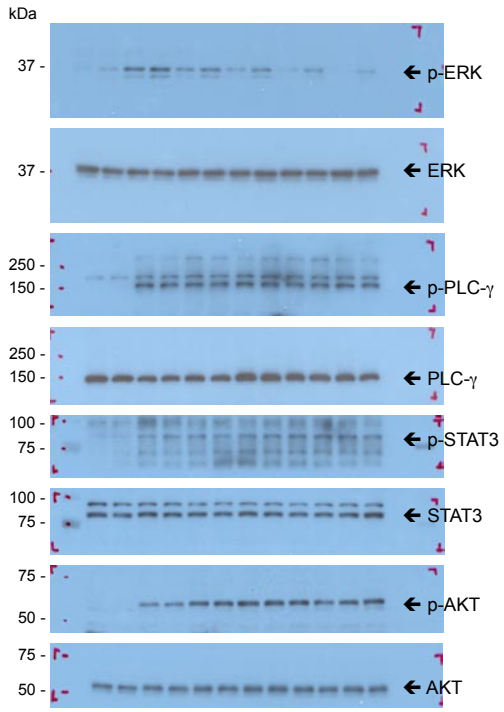

Fig. 5d

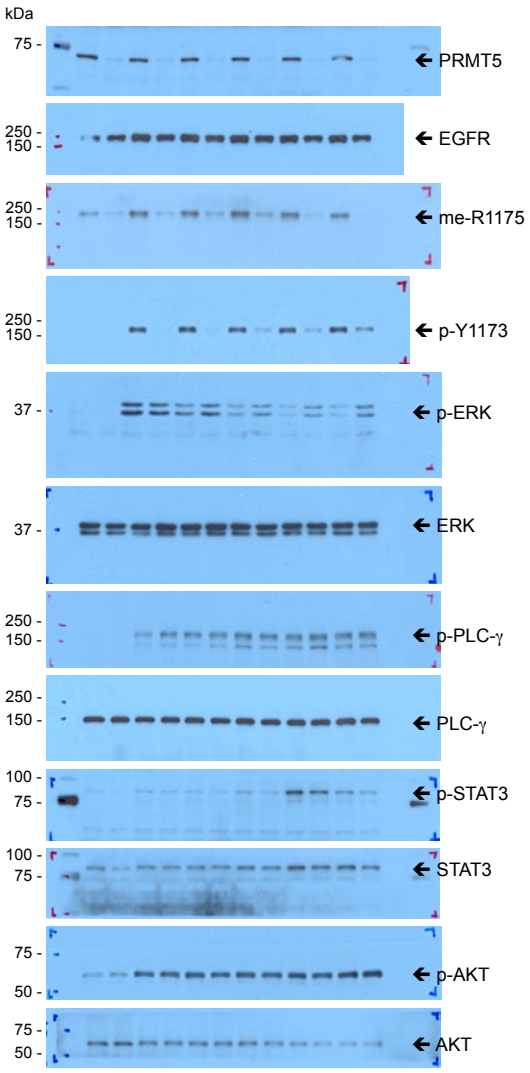

Figure S6 continued